ARCHITECTURAL RESEARCH, Vol. 11, No. 1(June 2009), pp. 15-23

Three-dimensional Topology Optimization using the CATO Algorithm

Sang Jin LEE and Jung Eun BAE
Engineering Research Institute, Gyeongsang National University
SJ·MIRAE & ADOPT Research Group, Department of Architectural Engineering, Gyeongsang National University

Abstract

An application of the constrained adaptive topology optimization (CATO) algorithm is described for three-dimensional topology optimization of engineering structures. The enhanced assumed strain lower order solid finite element (FE) is used to evaluate the values of objective and constraint functions required in optimization process. The strain energy (SE) terms such as elastic and modal SEs are employed as the objective function to be minimized and the initial volume of structures is introduced as the constraint function. The SIMP model is adopted to facilitate the material redistribution and also to produce clearer and more distinct structural topologies. The linearly weighted objective function is introduced to consider both static and dynamic characteristics of structures. Several numerical tests are tackled and it is used to investigate the performance of the proposed three-dimensional topology optimization process. From numerical results, it is found to be that the CATO algorithm is easy to implement and extremely applicable to produce the reasonable optimum topologies for three dimensional optimization problems

Keywords : CATO Algorithm, 3D Topology Optimization, Modal Strain Energy, Enhanced Assumed Strain, Solid Finite Element

1. INTRODUCTION

Over the last thirty years, topology optimization techniques have been extensively exploited and it became one of the most popular methods in engineering practice to produce the best possible topologies for various structures. The main idea of modern topology optimization technique is initiated by Cheung's work (1981) where the optimum thickness distribution of plate structures is investigated by using the regularization method. In the same context, Bendsoe and Kikuchi (1988) suggested the clearer means of resizing algorithm with homogenized method based on optimality criteria (OC) to redistribute the materials for planer structures. Later, the mathematical programming (MP) methods have also been used in topology optimization (Tenek and Hagiwara, 1993) together with the homogenized method but some limitations of the MP dealing with large scale problems are underlined again since the increase of the number of finite element (FE) causes the increase of design variables in topology optimization problems. Apart from OC and MP, several alternatives such as the hard-kill (Hinton and Sienz, 1995), the soft-kill (Walther and Mattheck, 1993) and the evolutionary method (Xie and Steven, 1997) have introduced in topology optimization process. In addition, the so-called constraint adaptive topology optimization (CATO) algorithm (Bulman and Hinton, 1999) is also proposed by the ADOPT research group with some important modifications on the kill methods.

Another main issue in topology optimization problems is the material model. Several important material models such as rank materials and polynomial material have been invented and those are applied into various topology optimization problems (Bendsoe, 1995; Hassani and Hinton, 1998). On the other hand, the so-called SIMP model (Bendsoe and Sigmund, 2004) has been also used in many topology optimization applications because of its versatility and generality. More rigorous and detailed descriptions on the development of both resizing algorithm and material model may refer to Reference (Bendsoe, 1995; Hassani and Hinton, 1998; Bendsoe and Sigmund, 2004).

In addition to the resizing algorithms and the material models, the use of three-dimensional FE techniques in topology optimization has been of great importance to deal with more realistic engineering problems. Diaz and Lipton (1997) presented a full relaxation strategy to find the optimal topology for three-dimensional elastic structures with minimum compliance. Olhoff et. al. (1998) suggested optimum three-dimensional microstructures for topology optimization of linear elastic three-dimensional continuum structures subjected to single load case. They showed that the MP technique based on the conventional design sensitivity analysis can be successfully used in three-dimensional topology optimization problems. They also provided a number of benchmark tests. Young et. al. (1999) deal with the implementation of bi-directional evolutionary method for three-dimensional topology optimization. Beckers (1999) developed a dual method where the design variables can only be zero and one values to deal with three dimensional problems. Fernandes et al. (1999) presented topology optimization methodologies for three-dimensional elastic bodies. Coelho et al. (2006) described a three-dimensional hierarchical model for topology optimization of structures. Hsu (2005) showed the method how to interpret three-dimensional structural topology optimization results. Campelo et al. (2007) suggested three-dimensional topology optimization results using an immune algorithm for electromagnetic design problem. James et al. (2008) introduced level set methods for three-dimensional structural topology optimization of an aircraft wing.

From literature review, we found that various three-dimensional topology optimization techniques have been proposed by many researchers in the wide range of disciplines including biomedical, automotive, aerospace and

architectural engineering. However, there has been no application of the CATO algorithm into three-dimensional problems although it has been validated as a simple and very effective way of redistributing the materials in two-dimensional problems. Therefore, we here describe the three-dimensional topology optimization procedures using the CATO algorithm and provide a series of benchmark tests to show the capability of the CATO algorithm in three-dimensional problems with consideration of both static and dynamic characteristics of the structures.

2. MATERIAL MODEL

It is reported that the homogenized material model often lead to blurred or in distinct grey scale density plots from which practical structural topologies must be discerned. This can lead to confusion and ambiguity on the part of the structural engineer in interpreting the optimal solution. Therefore, the SIMP model has been studied by several research groups (Lee et al., 2000; Rozvany, 2001) to overcome these difficulties and produce clearer and more distinct structural topologies. In the SIMP model, the material is characterized by a density parameter a_e which is usually used to define the material density $\rho_e = 1 - a_e^3$ in case of the cube cell having centrally placed cube holes.

Now, the elastic modulus E_e of the SIMP model in element e can be defined with the use of the material density ρ_e such as

$$\overline{E}_e = \rho_e^{\gamma} E_e \tag{1}$$

where the exponent γ usually has a value $0 \le \gamma \le 6$. Higher values of γ lead to more distinct topologies. From (1), it can be observed that the stiffness with SIMP model is varying associated with two parameters a_e and γ as shown in Figure 1. The density parameter a_e plays a role as design variables and γ will be used as a constant for entire optimization process.

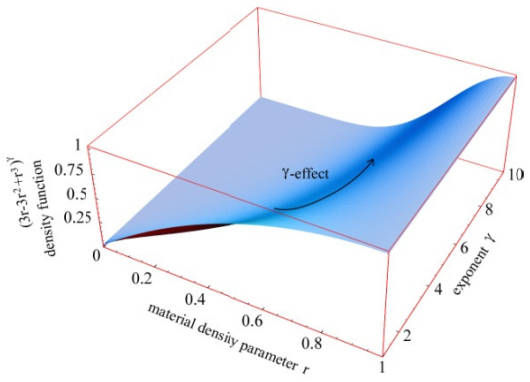

Figure 1. Material model: material density function with respect to the exponent γ

The volume V_e for the solid part of the element e can be defined as

$$V_e = \int_{\Omega_e} (1 - a_e^3)\, d\Omega = \rho_e \Omega_e \tag{2}$$

in which Ω_e is total volume of the FE.

3. CATO ALGORITHM

The CATO algorithm uses an incremental relationship $\Delta a_e^k(f_e)$ to adjust the elemental density parameter a_e according to the value f_e of each FE. In this study, the SE density of FE is used as the value of f_e. A special feature of this relationship is that it is chosen so as to preserve the total volume of the structure during the iterative optimization process. Here, we will briefly describe the essential procedure of the CATO algorithm necessarily required in three-dimensional topology optimization. Figure 2 shows an example of this relationship at two stages of the scheme.

The proposed function is composed of a curve of the form $y = ax^{\beta_k}$. In this study, the change in the density parameter Δa_e^k for element e at iteration k as shown in Figure 2 is given by

$$\Delta a_e^k = \alpha f_e^{\beta_k} \tag{3}$$

where

$$\alpha = -\frac{\Delta}{|\Delta|}, \Delta = f_e - f_{cut}, \hat{f}_e = {}^{\Delta}/_{\bar{f}}$$
$$\beta_k = \beta_0 - ((k - 1.0) \times \vartheta) \tag{4}$$

and f is defined as

$$\bar{f} = \begin{cases} f_{max} - f_{cut} & \text{if } f_e > f_{cut} \\ f_{min} - f_{cut} & \text{if } f_e \le f_{cut} \end{cases} \tag{5}$$

where β_0 is the initial curve exponent parameter, ϑ controls how the curve adapts through the iterative scheme.

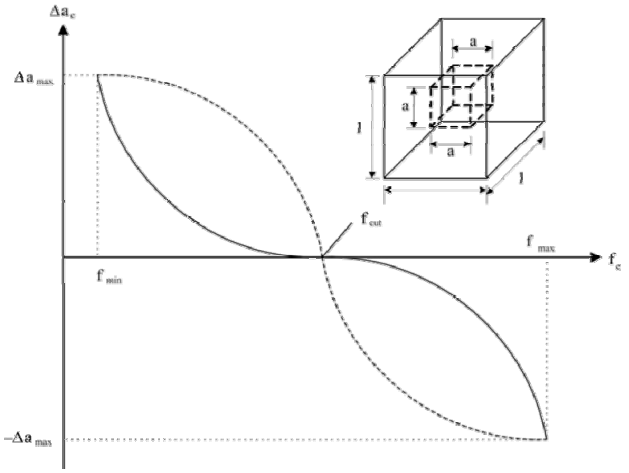

Figure 2. The relationship $\Delta a_e^k(f_e)$ at an early stage (solid line) of topology optimization iteration and at an intermediate stage (dash line)

After calculating the density parameters a_e^k for all elements, the volume of the new system is evaluated to check the volume equality constraint such as

$$\left|\frac{V_{sys}}{V_{des}} - 1\right| < V_{tol} \tag{6}$$

where V_{sys} is the volume of current system, V_{des} is the desired system volume and V_{tol} is some allowable tolerance on the volume constraint, typically less than 1%.

If (6) is satisfied, then the algorithm can proceed to the next iteration. However, if (6) is not satisfied then the volume error for each element is calculated as

$$V_{err} = \frac{V_{sys} - V_{des}}{nel} \tag{7}$$

where *nel* is the number of elements in the design domain and the new density parameter a_e^{k+1} for each element is calculated as

$$a_e^{k+1} = a_e^k + V_{err} \tag{8}$$

The overall CATO algorithm prescribed in the previous section is implemented as follows:

(a) Using a given volume fraction, calculate the initial value of design variables which are the density parameter

$$a_e^k = \begin{cases} 0 & \text{non design domain} \\ (1 - V_{fac})^{1/3} & \text{design domain} \end{cases}$$

(b) Evaluate the appropriate constitutive properties using SIMP model considering the current density parameter a_e^k

(c) Calculate the displacements u

(d) Calculate the SEs U_e

(e) Update the design variables using CATO resizing criteria

(e.1) Order the elements according to their SE density values

(e.2) From a specified volume preserving relationship $\Delta a_e^k(f_e)$, evaluate the change of the density parameters Δa_e^k, for each element and update the density parameter so that $a_e^{k+1} = a_e^k + \Delta a_e^k$

(e.3) Update the density parameters a_e. Note that the density parameter a_e is kept always above 0.0001 to avoid the instability of FE solution.

(e.4) Check whether new density parameters a_e are satisfied with the volume constraint

(e.5) If yes, go to (f). Otherwise, adjust a_e^{k+1} proportionately until the volume constraint is satisfied and then it is satisfied, go to (f)

(f) Filtering the density parameters if lower order FE is used whenever the option is on

(g) If the termination criterion (Lee et al., 2000) is satisfied, stop. Otherwise, repeat (b)-(f)

4. FILTERING (OR SMOOTHING) PROCESS

In engineering practice, the use of lower order FE is necessarily required to deal the large scale problem with many design variables. However, it is well-known that a checker-boarding appears in the final optimum topologies of the structures when the lower order FE is used in the topology optimization process. In this study, we therefore use a filtering technique to remove the checker-boarding phenomenon. The adopted technique is very similar to the stress smoothing which use a nodal average of stresses, i.e., the average of nodal stresses of all elements meeting at a common node. It means that we evaluate the nodal density parameter ρ_n by averaging the density parameters of all adjacent elements with the value of nel meeting at a target node n.

$$\rho_n = \frac{1}{nel}\sum_{e=1}^{nel} \rho_e \tag{9}$$

Finally, the smoothed element density parameter ρ_e for the 8-node solid FE are calculated by using the shape function N_a used in the displacement definition of 8-node solid FE (Lee and Lee, 2005) and nodal density parameter ρ_n as follows

$$\rho_e = \sum_{a=1}^{8} N_a \, \rho_n^a \tag{10}$$

The present filtering process will be active in the step (f) of previous section so that the checker-boarding phenomenon will be mitigated before the next iteration. Note that the filtering process described in this section has been used in the problem of two dimensional topology optimization problems (Youn and Park, 1997).

5. TERMINATION CRITERIA

In step (g) of Section 3, several termination criteria can be possibly used in the topology optimization. Four eligible termination criteria for the three- dimensional topology optimization can be summarized as follows:

(a) *The number of iterations*: A fixed number of iterations can be provided by user. The topology optimization will continue for the given number of iterations.

(b) *The SE norm*: The SE norm ($\left|U^k - U^{k-1}\right| / \left|U^{k-1}\right|$) between two subsequent topology optimization iterations will be examined and if the variation of SE between subsequent iteration is smaller than a given value then the algorithm will terminate.

(c) *The decrease percentage of SE*: If the SE of structure reach to the given SE value as ($U^k < U^0$), iteration will cease.

(d) *Volume changes*: If the volume change from one iteration to the next is less than a specified value then iteration will stop.

However, the first termination criterion is mainly used in the present study. The second termination criterion should not be used unless the decrease of SE is monotonic. From our experience, the first and the third and fourth termination criteria are recommendable when a new topology optimization problem is tackled.

6. STRAIN ENERGY TERMS

In the optimization process, we introduce linearly combined SE term which is generally considering m-load and n-natural frequency cases in the following form:

$$\bar{U} = \sum_{i=1}^{m} \lambda_i U^i + \sum_{k=1}^{n} \tilde{\lambda}_k \Phi \tilde{U}^k, \qquad \lambda_i, \tilde{\lambda}_k > 0 \quad (11)$$

where U^i, U^k are the elastic SE and the modal SE and the λ^i, λ^k are the associated weights with two SE terms U^i, U^k respectively. Note that we introduce an influence factor $\Phi_a = |U^a|/|U^k|$ to provide a physical meaning into the modal SE. The influence factor Φ_a can be determined in such way that the certain elastic SE term U^a is chosen by users.

More specifically, the elastic SE Term U^i induced by structural deformation associated the i^{th} load case can be calculated as

$$U^i = \left[\sum_{e=1}^{nel} \frac{1}{2} \int_v \varepsilon_e^T D \varepsilon_e \, dV \right]^i \quad (12)$$

where ε_e is strain vector and D is the rigidity matrix. In addition, the modal SE induced by the k^{th} eigenvector associated with the k^{th} natural frequency of the structures undergoing free vibration can be calculated as follows

$$U_m^k = \left[\sum_{e=1}^{nel} \frac{1}{2} \int_v \phi_e^T K_e \phi_e \, dV \right]^k \quad (13)$$

Where ϕ_e is the eigenvector associated with element e.

In the optimization process, the values of SE for all FEs are calculated by using (11) and it is finally sorted in the ascending order for the CATO algorithm.

Note that the SE values of the FEs discretized in the structures are calculated by enhanced lower order solid FE and its detailed formulation is described in Reference (Lee and Lee, 2005).

7. NUMERICAL EXAMPLES

In order to show the performance of the proposed three-dimensional optimization technique, a set of benchmark tests is introduced. Several important aspects of the SIMP model and the CATO resizing algorithm are carefully tested. The parameters and aspects used in the benchmark tests can be summarized as follows:

(a) Resizing algorithm: the initial curve exponent parameter β_0, the curve adaptation parameter,
(b) The effect of volume fraction V_f,
(c) SIMP model: the exponent of the material density,
(d) Multi-objective cases: consideration of both elastic SE and modal SE.

Each parameter is tested individually to show its effect on the process of topology optimization. However, it should be noted that the other parameters are fixed at certain specified values when one parameter is tested. Note that with the form of topology optimization used here based on linear elastic behaviour, the optimum topology obtained is, of course, independent of the value of the elastic modulus and load intensity. In the studies, specific values for the elastic modulus, load intensity and design domain dimension are provided. However, in all convergence plots normalized strain energy is used for clarity. Checker-boarding of optimum topologies has been identified as a problem in topology optimization using 8-node lower order solid FE and the filtering process described in Section 3 used to avoid checker-boarding.

7.1 CANTILEVER BEAM: THE PARAMETERS AND VOLUME FRACTION USED IN CATO ALGORITHM

The cantilever beam subjected to a point load at the top of the right hand-side edge is optimized. The dimensions of the rectangular design domain are L=16.0m, H=10.0m and thickness normal to plane of structure t=1.0m. The following material properties are assumed: elastic modulus E=1.0 $\times 10^5$ N/m^2 and Poisson's ratio υ =0.3. The volume is constrained to be equal to $\Omega = 30\%$ of the total volume of the beam and the magnitude of the load is P=10kN. The analysis is carried out using 640, 8-node solid FEs. Note that the exponent γ of the SIMP model is taken as 5.0. In this example, two important optimization parameters used in the CATO resizing algorithm are investigated.

First, the effect of changing the curve exponent β_0 on the rate of convergence is investigated. In this case, values of 0.01 for the curve adaptation parameter ϑ and 0.0001 for the volume tolerance are used. After 100 iterations, the SE reductions of 99%, 97%, 87%, 81% and 78% are achieved for the curve exponent β_0= 1.0, 3.0, 5.0, 7.0 and 9.0 respectively. It means that a faster convergence rate can be achieved with a larger value of the curve exponent. The convergence curves are presented in Figure 3.

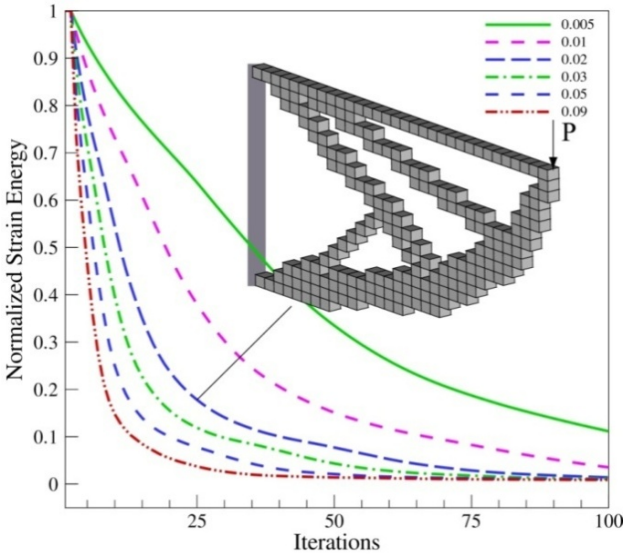

Figure 3. The rate convergence with respect to the curve exponent β_0

Second, the effect of changing curve adaptation parameter ϑ on the rate of convergence is considered for the curve exponent value of 0.01 and a volume tolerance of 0.0001. Because of a large value of the curve adaptation parameter used in this example, the SE reduction of approximately 99% is achieved after 100 iterations for all cases except for the cases with curve adaptation parameters of 0.01, 0.005 which give 96% and 89% SE reduction. This result indicates that larger values of the curve adaptation parameter accelerate the topology optimization process. The convergence curves are presented in Figure 4.

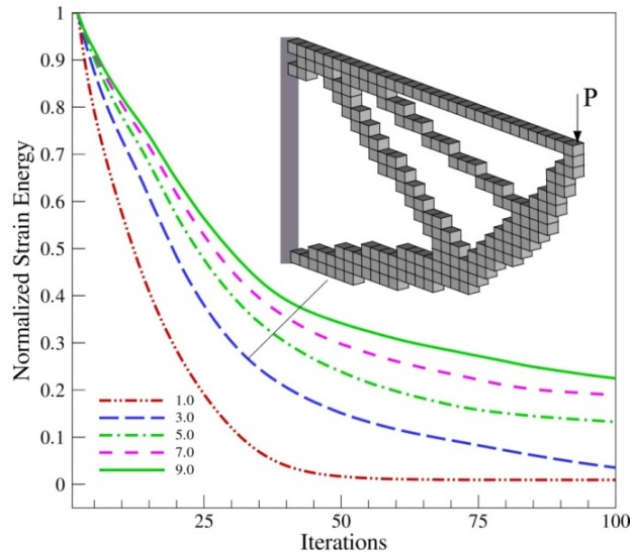

Figure 4. The rate convergence with respect to the curve adaptation parameter ϑ

It should be noted that the rate of convergence may change if a different material such as the homogenized microcell material is adopted. Additionally, the effect of changing different volume fraction V_f on the optimal topologies is examined. In this case, the curve exponent β_0 the curve adaptation parameter ϑ and the tolerance of volume have fixed values equal to 0.8, 0.04 and 0.0001 respectively. Figure 5 shows the resulting optimal topologies for values of volume fraction V_f ranging from 10% to 90%.

Figure 5. Topology with respect to different volume fractions (V_f) : (a) 10%, (b) 20%, (c) 30%, (d) 40%, (e) 50%, (f) 60%, (g) 70%, (h) 80% and (i) 90% of the volume of the initial configuration of the beam

7.2 SIMPLY SUPPORTED BEAM: SIMP MODEL

The behavior of the SIMP model is highly dependent on the exponent value γ of (1). Specifically, the order (or value) of the elastic modulus function is directly determined by the value of the exponent as shown in Figure 1. The simply supported beam is used to investigate the effect of exponent value γ on topology optimization. The dimension of beam are L=2.0m, H=1.0m and thickness normal to plane of structure t=1.0m. The material properties used in this example are elastic modulus E=1.0 $\times 10^5$ N/m^2 and Poisson's ratio υ =0.3. The volume is constrained to be equal to $\Omega = 40\%$ of the total volume of the beam and the magnitude of a central point load is P=10kN. The analysis is carried out using 1800, 8-node solid FEs. The fixed values of the optimization parameters used in the optimization are the curve exponent $\beta_0 = 5.0$, the curve adaptation parameter $\vartheta = 0.01$. The volume tolerance of 0.001 is used. In this example, a range of exponents from γ=0.2 to γ=9.0 is investigated. From numerical results, optimum topologies are found to be sensitive to the different range of γ. In particular, poor topologies are observed for the value of less than $\gamma = 1.0$. Although larger values of the exponent can trigger poor results with small values of the volume fraction as reported in Reference (Lee et al., 2000), this situation can be improved if larger value of the volume fraction such as the present value of 40% is used. The results obtained from the use of different values of the exponent are presented in Figure 6. We can see that the final topology with CATO algorithm can be significantly affected by the exponent of the SIMP model.

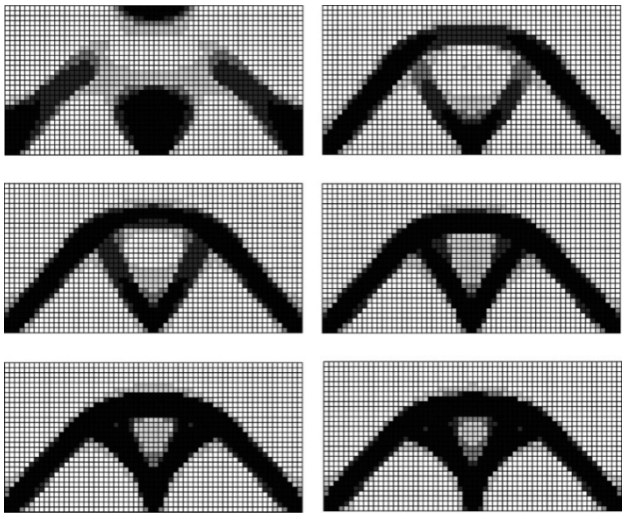

Figure 6. Topologies with respect to different values of the exponent of the artificial material model: (a) $\gamma = 0.2$, (b) $\gamma = 2$, (c) $\gamma = 3$, (d) $\gamma = 5$, (e) $\gamma = 7$ and (f) $\gamma = 9$

7.3 CLAMPED SQUARE PLATES: DIFFERENT BOUNDARY CONDITIONS

Square plates with different boundary conditions are optimized with the objective minimizing modal SE by using the proposed three-dimensional topology optimization technique. The four sides of the square plate can have various combinations of boundary conditions. The four boundary conditions C/C/C/C, C/F/C/F, C/F/C/C, F/F/C/C are used in this example as shown in Figure 7.

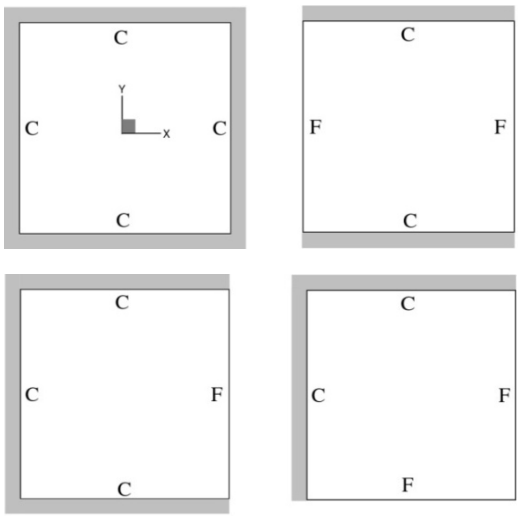

Figure 7. Square plate: Models used for (a) C/C/C/C, (b) C/F/C/F, (c) C/F/C/C and (d) F/F/C/C boundary conditions

The C and F denote clamped and free boundary conditions respectively. For concise identification, the cases are denoted by four letters which stand for each of the four sides in the rectangular plate. This sequence begins with the side corresponding to lower edge and proceeds anti-clockwise around the plate. The side length of the plate is a=4.0*m* and the total thickness of plate is h=0.2*m*. The material properties used in this example are assumed to be: elastic modulus $E = 3.2 \times 10^7 N/m^2$, Poisson's ratio $\nu = 0.3$. A volume fraction of $\Omega = 50\%$ is used and the following solution parameters $\beta_0 = 5.0$, $\vartheta = 0.025$ are used for CATO algorithm. The tolerance of the volume fraction is 0.001. The exponent of the artificial material is taken as 5.0. A mesh of 900, 8-node solid elements is used for the FE analysis in full structure. In this test, 100 iterations are allowed and the filtering process is continuously applied until 100 iterations. We mainly consider the minimization of modal SE associated with the fundamental mode shape of the plate. Figure 8(right) provides the optimum topologies obtained from the minimization of the modal SE distribution induced by the fundamental mode shapes shown in Figure 8(left).

From numerical results, it is observed that the optimized plates have achieved 58%, 36%, 67%, 65% of the modal SE reductions. From a practical point of view, the dark area of the topology optimization result may be considered as the area where reinforcement is required to effectively resist the natural mode shape.

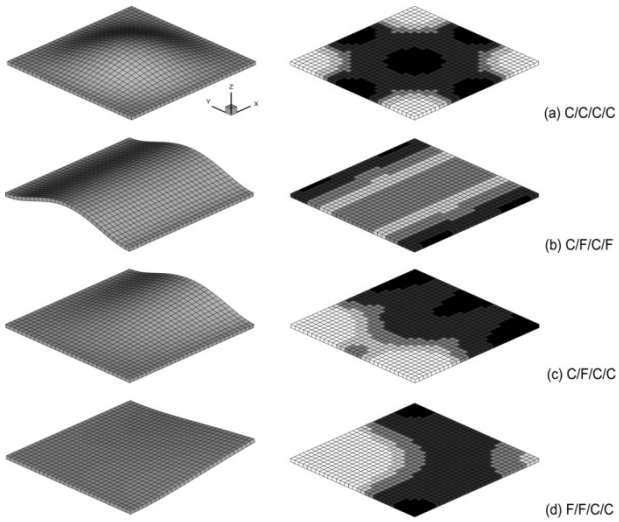

Figure 8 The fundamental mode shapes and optimum topologies of the square plates with different essential boundary conditions such as: (a) C/C/C/C, (b) C/F/C/F, (c) C/C/F/C and (d) F/F/C/C

7.4 DOUBLY CURVED SHELL: MULTI-OBJECTIVE FUNCTION

A doubly curved shell subjected to a central point load is optimized. The four corners of the shell are clamped. The geometry of the shell is expressed by the equation:

$$z = \frac{C(x^2 + y^2)}{(L/2)^2}$$

in which C=L/10 and L=6m and the initial shape of the shell is presented in Figure 9.

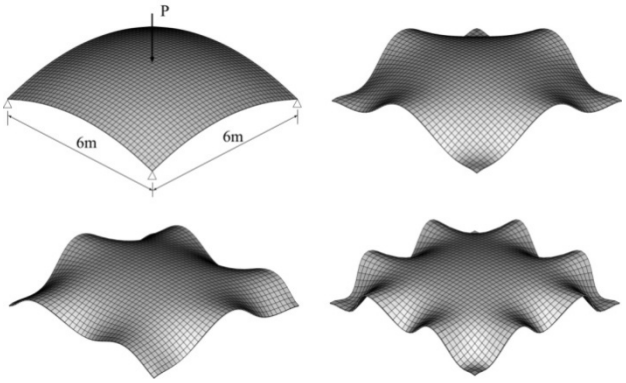

Figure 9. Doubly curved shell. Left-top: geometry, right-top: the first mode shape, left-bottom: the second mode shape and right-bottom: the third mode shape

The material properties used in this example are assumed to be: elastic modulus$E = 3.2 \times 10^7 N/m^2$, Poisson's ratio $\nu = 0.3$ and the thickness of shell is $h = 0.2m$. A mesh of 400, 8-node solid elements is used for the FE analysis in a symmetric quadrant. A volume fraction of $\Omega = 50\%$ is used and the parameters $\beta_0 = 5.0$, $\vartheta = 0.025$ are used for CATO algorithm. The exponent γ of the SIMP model is taken as 5.0. The tolerance of the volume fraction is 0.001. In this test, 250 iterations are allowed and the filtering process is applied until 150 iterations. Note that only symmetric modes of the shells described in Figure 9 are considered in the optimization process. In this test, the multi-objective problem is tackled and therefore the external load $P = 10kN$ and natural mode shapes shown in Figure 9 are simultaneously considered in topology optimization process. Four cases are considered: (a) P, (b) ω_1, (c) $P + \omega_1$, (d) $P + \omega_3$. In the first case, we try to obtain the optimum topology against a central point load. The first modal SE minimization is then tackled in the second case. Furthermore, multi-objective problems are considered in the other cases.

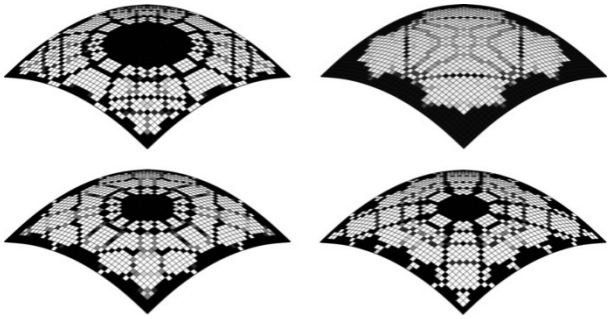

Figure 10. Optimum topologies for doubly curved shell. Left-top: point load, right-top: the first mode shape, left-bottom: point load and the first mode shape and right-bottom: point load and the third mode shape

Figure 10 provides the optimum topologies obtained from the single-objective and multi-objective cases. In particular, for the multi-objective problems, modal SE is normalized and its level is then adjusted to that of elastic SE with the use of influence factor defined in Section 6. The unit weight is used to define the linearly combined total SE for shell. For example, the weights and total SE for the third case are used as $\lambda_1 = \tilde{\lambda}_1 = 1$ and $\bar{U} = \lambda_1 U_1 + \tilde{\lambda}_1 \Phi_1 \tilde{U}_1$. From numerical results, it is observed that the material of shell is re-distributed and a discrete structure is evolved to resist the deformation induced by external load or/and the natural mode shapes. The total SE reduction of 82%, 81%, 70%, 72% are achieved for the present four cases. It is also found to be that the final optimum topologies of the shell have been greatly affected by the implicit consideration of the dynamic characteristics of the shell in the form of modal SE.

7.5 THREE DIMENSIONAL STRUCTURES

The proposed technique based on the CATO algorithm is also tested by using three-dimensional structures described in Reference (Olhoff et al., 1998). Two structures such as cantilever beam and cube structure are used in this test and the dimensions of two structures are illustrated in Figure 11. The following material properties are assumed: elastic modulus E=2.1 $\times 10^{11}$ N/m^2 and Poisson's ratio $\upsilon = 0.0$. For the cantilever beam as shown in Figure 11(left), the volume is constrained to be equal to $\Omega = 40\%$ of the total volume of the design domain and the magnitude of the load is P=1N. The analysis is carried out using 1500, 8-node solid elements. For the second cube structures as shown in Figure 11(right), the volume is constrained to be equal to $\Omega = 20\%$ of the total volume of the design domain and four parallel point loads P=10 N are applied at the upper surface. The analysis is carried out using 2000, 8-node solid elements which is discretized in the quarter of the design domain. Note that the exponent γ of the SIMP model is taken as 5.0. The curve exponent $\beta_0 = 5.0$ and the curve adaptation parameter ϑ=0.025 are used. The optimum topologies for two adopted three-dimensional design domains are illustrated in Figure 11.

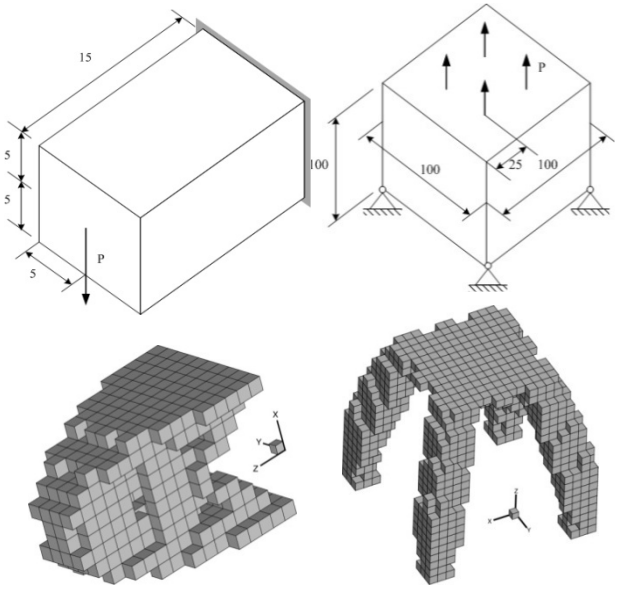

Figure 11. Problem definition and optimum topologies for three- dimensional problems. Left: cantilever beam, right: cubic domain

For cantilever beam, its optimum topology is obtained with the section of I-beam to effectively resist the bending moment induced by tip point load. For cube structure, its optimum topology consists of four legs and each of leg tends to transfer the applied concentrated loads to the nearest support. It is found to be that the present solution has a good agreement with the reference solutions (Olhoff et al., 1998).

8. CONCULSION

Three-dimensional topology optimization technique based on CATO algorithm is proposed to find optimum topologies for engineering structures. It is found to be that the present technique is proven to be simple and extremely applicable to the design optimization problems trying to minimize both elastic and modal SEs of the three-dimensional structures. We also found that the proposed technique can be effectively utilized to find various discrete structures which can be considered as the alternatives to continuum structures. A set of benchmarks are provided to show the capability of the proposed methodology on three-dimensional topology optimization. Here, some specific conclusions are now drawn from the benchmark tests:

(1) The recommended value of the curve exponent β_0 is in the range from 5.0 to 9.0 when the CATO algorithm is used for three-dimensional structures.
(2) The recommended value of the curve adaptation parameter ϑ is in the range from 0.01 to 0.09 when the CATO algorithm is used.
(3) The value of the exponent in the SIMP model plays an important role in topology optimization as shown in Section 7.2. From this study, a value in the range from 3.0 to 5.0 for the exponent is a recommended for most cases.
(4) The adopted filtering process can effectively avoid checker-boarding without any difficulty.
(5) The SIMP model is simple and very effective and it can produce a very good layout for most structures.
(6) The proposed methodology based on CATO algorithm can provide a good performance and a stable convergence in three-dimensional structures for most cases.

ACKNOWLEDGEMENTS

The research grants from the EPSRC (GR/K22839), UK and the Ministry of Construction & Transportation, Korea, for the Construction Technology Research & Development Program (PN: 06-R&D-B03) are gratefully acknowledged.

REFERENCES

Beckers, M. (1999) "Topology optimization using a dual method with discrete variables." *Structural Optimization,* 17: 14-24.

Bendsoe, M.P. (1995) *Optimization of structural topology shape; and material*. Springer-Verlag.

Bendsoe, M.P. & Kikuchi, N. (1988) "Generating optimal topologies in structural design using homogenization method." *Computer Methods in Applied Mechanics and Engineering*, 71: 197-224.

Bendsoe, M.P. & Sigmund, O. (2004) *Topology optimization*, Springer-Verlag.

Bulman, S.D. & Hinton, E. (1999) "Constrained adaptive topology optimization of engineering structures." *Design Optimization*, 1: 419-439.

Campelo, F., Watanabe, K. & Igarashi, H. (2007) "3D topology optimization using immune algorithm." *International Journal for Computation and Mathematics in Electrical and Electronic Engineering,* 26(3): 677-688.

Cheng, G. & Olhoff, N. (1981) "An investigation concernng optimal design of solid elastic plates." *International Journal of Solids and Structures*, 17: 305-323.

Coelho, P.G., Fernandes, J.B., Cardoso, J.B., Guedes, J.M. & Rodrigues, H.C. (2006) "A three-dimensional hierarchical model for topology optimization of structures." In Proceedings of the 3rd European Conference on Computational Mechanics Solid, Structures and Coupled Problems in Engineering, Lisbon, Portugal, 5-8.

Diaz, A. & Lipton, R. (1997) "Optimal material layout for 3D elastic structures." *Structural Optimization*, 13: 60-64.

Fernandes, P. R., Guedes, J.M. & Rodrigues, H. (1999) "Topology optimization of 3D linear elastic structures." *Computers & Structures*, 73: 583-594.

Hassani, B. & Hinton, E. (1998) *Homogenization and Structural topology optimization*, Springer-Verlag.

Hinton, E. & Sienz, J. (1995) "Fully stressed topological design of structures using an evolutionary approach." *Engineering Computations*, 12: 229-244.

Hsu, M. & Hsu, Y. (2005) "Interpreting three-dimensional structural topology optimization results." *Computers and Structures*, 83: 327-337.

James, K.A., Martins, J.R.R.A. & Hansen, J.S. (2008) "Three-dimensional structural topology optimization of an aircraft wing using level set methods." In Proceedings of the 12th AIAA/ISSMO Multidisciplinary and Optimization Conference, Victoria, British Columbia, Canada, 1-12.

Lee, S.J., Bae, J.E. & Hinton, E. (2000) "Shell topology optimization using layered artificial material model." *International Journal for Numerical Methods in Engineering*, 47: 843-867.

Lee, S.J. & Bae, J.E. (2006) "The strain energy based topology optimization technique maximizing the fundamental frequency of the structures." In Proceedings of the 10th East Asia-Pacific Conference on Structural Engineering & Construction (EASEC-10): Analytical and Computational Methods, Bangkok, 229-234.

Lee, S.J. & Lee, Y.J. (2005) "A comparative study on the free vibration analysis of shell structures with lower order solid finite elements." *Journal of the Architec-*

tural Institute of Korea, 21(4): 39-46.

Olhoff, N., Ronholt, E. & Scheel, J. (1998) "Topology optimization of three-dimensional structures using optimum microstructures." *Structural Optimization*, 16: 1-18.

Rozvany, G. I. N. (2001) "Aims, scope, methods, history and unified terminology of computer-aided topology optimization in structural mechanics." *Structural and Multidisciplinary Optimization*, 21(2): 90-108.

Tenek, L.H. & Hagiwara, I. (1993) "Static and vibrational shape and topology optimization using homogenization and mathematical programming." *Computer Methods in Applied Mechanics and Engineering*, 109: 143-154.

Xie, Y.M. & Steven, G.P. (1997) *Evolutionary structural optimization*, Springer-Verlag.

Youn, S.K. & Park, S.H. (1997) "A study on the shape extraction process in the structural topology optimization using homogenization material." *Computers & Structures*, 62: 527-538.

Young, V., Querin, Q.M., Steven, G.P. & Xie, Y.M. (1999) "3D and multiple load case bi-directional evolutionary structural optimization (BESO)." *Structural Optimization,* 18: 183-192.

Walther, F. & Mattheck, C. (1993) "Local stiffening and sustaining of shell structures by SKO and CAO." In Proceeding of International Conference on structural optimization, Edited by C.A. Brebbia and S. Hernandez, 181-188, Computational Mechanics, Southampton, UK

(Data of Submission : 2009.1.4)